The Electrical Conductivity in Argon Potassium and Helium Potassium Plasmas with Elevated Electron Temperatures in Crossed Electric and Magnetic Fields

G. Brederlow, R. Hodgson

IPP 3/59 September 1967

INSTITUT FÜR PLASMAPHYSIK

GARCHING BEI MÜNCHEN

INSTITUT FÜR PLASMAPHYSIK

GARCHING BEI MÜNCHEN

The Electrical Conductivity in Argon Potassium and Helium Potassium Plasmas with Elevated Electron Temperatures in Crossed Electric and Magnetic Fields

G. Brederlow, R. Hodgson

IPP 3/59 September 1967

Die nachstehende Arbeit wurde im Rahmen des Vertrages zwischen dem Institut für Plasmaphysik GmbH und der Europäischen Atomgemeinschaft über die Zusammenarbeit auf dem Gebiete der Plasmaphysik durchgeführt.

IPP 3/59 G. Brederlow
R. Hodgson

The Electrical Conductivity in Argon Potassium and Helium Potassium Plasmas with Elevated Electron Temperature in Crossed Electric and Magnetic Fields.

September 1967 (in English)

Abstract

Methods and results of measurements of the tensor conductivity and electron temperatures in argon potassium and helium potassium plasmas with elevated electron temperatures under MHD generator conditions are described. Electrode and wall effects that would make the measurements more difficult to interpret have been eliminated. Calculations of W. Feneberg predict that the scalar electrical conductivity should drop slightly with increasing magnetic field strength. However, the measured effective scalar conductivity was less than the theoretically predicted value. The discrepancy is apparently due to instabilities. These instabilities were investigated. At current densities and field strength values at which instabilities were observed, the effective Hall coefficient has been found to be nearly independent of the magnetic field strength.

The measurements have shown that the efficiency of a noble gas MHD generator is adversly affected not only by the decrease of the scalar conductivity in a magnetic field, which has been predicted by W. Feneberg, but also by the onset of instabilities.

I. Introduction

The enhancement of the electrical conductivity of the working gas in magnetohydrodynamic generators by increasing the electron temperature as first proposed by J.L. Kerrebrock [1] has been experimentally investigated by various groups [1 - 6]. The measurements were carried out in a mixture of rare gas and alkali metal under conditions approximating those in MHD generators, but the "non equilibrium" ionization was induced by an applied external electric field and not by the $\vec{v} \times \vec{B}$ e.m.f. The results confirmed the two-temperature plasma model proposed by J.L. Kerrebrock. However, in experimental MHD generators using $\vec{v} \times \vec{B}$ e.m.f. to elevate the electron temperature in the rare gas alkali metal mixture, a performance as high as expected from the two-temperature model, and from the results of experiments with no magnetic field, has not been achieved.

These disappointing results could have many causes. For example, voltage drops at the electrodes, geometry factors associated with the segmented electrodes of MHD generators [7 et al.], current concentrations at the electrode walls at high values of the Hall parameter $\beta = \omega\tau$ [8], eddy currents in the plasma, and short circuiting of adjacent and opposed electrodes through the insulating material could be responsible for the failure of many experimental generators. Both phenomena such as instable fluctuations [9, 10, 11 et al.] and the effect of the magnetic field on the electrical scalar conductivity [12, 13] could also reduce generator performance.

In most of the existing generators it is difficult or impossible to investigate these effects separately or, in fact, to do more than guess at the cause of the disparity between theory and experiment. Therefore, we have used a slightly different experimental arrangement in order to investigate the bulk plasma phenomena in an argon potassium and helium potassium plasma and eliminated most of the effects that disturb MHD generator measurements. We have kept MHD generator conditions (i.e. crossed electric and magnetic fields), but induced the current flow by an electric field applied in the direction of the gas flow. The electrical conductivity and electron temperature could then be measured (in a region free from electrode effects) as functions of current density and applied magnetic field.

II. Apparatus

In order to carry out detailed and accurate investigations of the elevation of the electron temperature and the electrical conductivity under steady state MHD generator conditions, we used the noble gas potassium plasmas under controlled conditions of purity, temperature, and composition.

A schematic diagram of the apparatus is shown in Fig. 1. The gas is heated by two arc heaters and mixed with potassium vapour in a mixing chamber. The mixture then flows through a measurement channel to a heat exchanger where it is cooled down. The potassium is then filtered out and the pure gas may be vented to the atmosphere or returned to a compressor to be recycled.

The entire system is designed to be free of impurities and to give trouble free, long life service. Boron nitride encased in magnesium oxide are used for heat and electrical insulation. Rubber or copper O-rings between the various parts of the stainless steel outer casing ensure that it remains vacuum tight. Only the flanges containing rubber O-rings are cooled.

To heat the gas without introducing impurities, two arc heaters with tungsten cathodes and water cooled copper anodes are used. They may be run with 20 kW input power for more than a hundred hours without showing erosion.

The jet from each arc heater is directed axially into a mixing chamber. Tungsten pipes protect the BN insulation tubes from uneven heating. A special arrangement has been developed for supplying potassium so that it is added to the hot gas as a steady, exactly known and adjustable vapour flow. The liquid potassium, which is contained in a heated cylinder, is pushed into the bottom of an evaporation chamber by a variable speed piston (Fig. 2). The evaporation chamber is made from a 0.6 cm I. D. tungsten cylinder (with the top end blocked off) which projects into the mixing chamber. A 0.2 mm hole is drilled in the closed end of the tungsten cylinder. Excess pressure builds up in the evaporation chamber until the rate of vapour flow through the hole equals the feed rate. With this system, the irregularities in the potassium supply caused by unsteady evaporation at the potassium liquid-vapour interface and by irregular piston motion are cut down.

After passing through the measuring channel, the rare gas potassium mixture is cooled down to 80 °C in a water cooled heat exchanger. Since condensation centres are absent in the very pure mixture, a supersaturated potassium vapour component is left in the gas and must be filtered out. We have found that glass wool is very effective for this purpose. Since the potassium "wets" the glass a large surface area of liquid potassium is able to form and provides the needed condensation centres. Most of the potassium condenses out within several millimetres of the filter surface, and runs down on the surface to the bottom of the filter housing. This potassium may then be collected and reused, and the filter does not block up.

III. The measuring channel and diagnostic devices

The measuring channel housing is constructed to allow maximum freedom of choice of diagnostic methods and channel geometries, combined with ease of assembly and disassembly.

Air core magnetic field coils were chosen to provide free access for optical diagnostics. They provide a field strength of 20 kG with 5 % non-uniformity over the channel.

The channel itself has a cross section 15 x 20 mm^2 and is 100 mm long. It is made from BN blocks fitted flush together. Extra thermal insulation is provided by a 5 cm layer of MgO chips between the outside of the BN and the stainless steel walls of the housing.

In order to prevent potassium from diffusing out from the channel and short circuiting the electrical leads, all BN joints are coated on the outside with a paste that hardens into a high temperature resistant solid. In addition, the space between the housing and the channel walls is kept at a slight overpressure (with respect to the channel pressure).

Fig. 3 shows one of the geometries we have used for the measuring channel. Direct current was sent through the channel in the direction of the gas flow through the Ta electrodes at each end. The electron temperature T_e and the conductivity σ could then be measured under

the essential MHD generator conditions (i.e. crossed electric and magnetic fields) in a region free of electrode effects.

Tungsten wires with a diameter of 0.5 mm strung across the channel in the direction of the magnetic field B and tantalum electrodes imbedded in the walls were used to measure the potential distribution. The windows in the insulated side allow observation through the channel in the direction of B. The distribution of T_e over the channel height y was measured through these windows.

The plasma in the measuring channel is in good electrical contact with the outer casing through the nozzle of the potassium injection system which projects into the plasma. To prevent the measuring current from flowing partly from the upstream electrodes through the nozzle over the housing to the exhaust and hence back to the downstream electrodes in the channel the plasma on the downstream side of the channel was carefully insulated from the housing until it was quenched. In addition, the housing, the anodes and the cathodes of the arc heaters were insulated from one another and from the ground.

Most experiments were carried out with a gas temperature of T_g = 2000 ^{o}K, gas pressure of p = 1.16 atm., flow velocity of v = 190 m/sec and a potassium seed concentration of c = 0.3 % K.

The measured velocity and gas temperature profiles were nearly constant up to about one millimetre from the wall. We could continue the experiment for hours, and so equilibrium conditions were always reached.

The gas temperature distribution was checked with a movable W • 3 % R / W • 25 % R thermocouple. The electron temperature was measured using the line reversal method. Light from a tungsten strip lamp transmitted through the plasma plus the light emitted from the plasma is focussed on one end of a light pipe. This end could be transversed in the focal plane where the image of the plasma, projected through the side windows, was built up. In this way one could measure the light intensity coming from different points in the channel. The image of the excit slit is then projected on the entrance slit of a Zeiss MG 4 monochromator. The light is finally passed through to a cooled and heavily

shielded RCA 7102 photomultiplier. The signal from the photomultiplier is filtered and amplified, and used to record the intensity I_λ of the radiation coming from the windows on the y axis of an oscilloscope or an x-y recorder. The x axis may record the wavelength λ setting of the monochromator. The radiation intensity from the strip lamp $B_\lambda(T_B)$ incident in the channel (measured directly with a photocell), or the position y of the end of the light pipe.

Fig. 4 shows a plot of I_λ vs λ for different background source intensities B_λ (T_B). Since the plasma is very optically thick to the resonance line radiation, the lines are very broad and can be resolved by a simple instrument [14].

It could be shown that the reversal temperature equals the electron temperature in an argon potassium plasma only when the energy lost by the plasma by resonance radiation to the walls is very much less than the energy exchanged in electron collision processes between the upper and lower states corresponding to the resonance line [15]. Fig. 4 shows that the optical thickness is so large that most of the resonance radiation is trapped in the plasma, and the above condition is fulfilled.

In fact, the plasma is so optically thick that the radiation in the line middle comes only from the colder zones near the wall. The radiation from the hotter plasma in the middle of the channel is completely absorbed except in the wings of the line, where the plasma is more transparent to the radiation. We may thus use the line middle to measure the reversal temperature near the wall, but we must use the radiation in the line wings, where the plasma is nearly transparent, to measure the temperature in the middle of the channel.

The maximum difference between the reversal temperatures measured using the radiation in the line wings and the line middle was 100 ^{o}K. In the following sections, temperatures measured using the wings of the line will be quoted.

The total radiation intensity of the emission lines may be calibrated to find T_e. Fig. 5 shows $\log \int I_\lambda \, d\lambda$ measured by opening the mono-

chromator slit to integrate over both potassium resonance lines plotted as a function of the measured $^1/T_e$. Calibration curves of this type were used to convert the measurements of I_λ as a function of y to curves of T_e as a function of y.

The conductivity tensor must be calculated from the electric field in the plasma and the current density. We have derived the electric field vector from the potential distribution in the channel. The voltages between the 20 probes were recorded simultaneously on photographic paper by means of two Siemens light beam oscillomats. Each channel had 100 kΩ input impedance and 100 Hz frequency response. In this way, a picture of the effect of current density on the potential distribution could be obtained. Fig.6 shows such a potential distribution with and without a magnetic field.

If the current is restricted to flow only in the x direction, (i.e. the direction of the flowing gas) so that $j_y = 0$, the scalar conductivity σ_o can be found by dividing the current density j_x by the x component of the electric field E_x. Also, if the $(\vec{v} \times \vec{B})$ e.m.f. is taken into account the Hall coefficient $\omega\tau$ can be derived from the electric field components E_x and E_y. One obtains:

$$\sigma_o = \frac{j_x}{E_x} \quad \text{and} \quad \omega\tau = \frac{E_y^*}{E_x^*} = \frac{E_y - v_x B_z}{E_x} \qquad (1)$$

If $j_y \neq 0$, an additional e.m.f. $\frac{1}{n_e e} \cdot j_y B_z$, which opposes the applied electric field, is induced in the x direction. The scalar conductivity and the Hall coefficient may then no longer be calculated so simply.

At first we found that the current density distribution in the test section was not uniform when the current was sent into the channel through only one pair of electrodes. Fig. 7 shows a computer solution for the current density in this case when a magnetic field is applied to a simulated channel [16]. The extreme non-uniformity is due to the distribution of the current density at the electrode surface in a high $\omega\tau$ plasma. It is analogous to the electrode effects observed in MHD generators with segmented electrodes. Computer analysis showed

that the current density distribution may be made uniform and j_y made zero by staggering the electrodes and moving them further apart. We have used three independent circuits to send currents through staggered electrodes and have succeeded in making the current density uniform in the test section.

The uniformity of the current density direction was checked by measuring the uniformity of $\vec{E}$. The vectors $\vec{j}$ and $\vec{E}^* = \vec{E} + \vec{v} \times \vec{B}$ form a fixed angle $\Theta = \arctan \omega\tau$ with one another. Since Θ is relatively insensitive to the absolute value of j, the direction of $\vec{E}$ is a sensitive indicator of the direction of $\vec{j}$, but not of the absolute value of j. Therefore, the current distribution may be anisotropic in spite of a uniform $\vec{E}$ distribution.

To eliminate this possible source of error from our conductivity measurements, we have measured the light intensity (which is a very sensitive function of the electron temperature T_e and thus of the current density $|j|$) emitted through the side windows as a function of the channel height y. These measurements combined with the electric field measurements made it possible to adjust the current distribution until it was homogeneous.

Eddy currents in the plasma must be checked to see that the j_y components do not disturb the measurements. For no eddy currents to flow, both the $\frac{1}{n_e e} j_x B_z$ and the $v_x \times B_z$ e.m.f.'s must be constant in the test section so that they are exactly compensated by an electrostatic field E_y. In addition, the side walls must be perfect insulators to prevent current from flowing and reducing the E_y field. We have investigated possible disturbances caused by variations in the e.m.f.'s and finite wall conductivity.

The currents circulating entirely in the plasma under the influence of the $\vec{v} \times \vec{B}$ force were estimated from the calculated velocity, temperature and conductivity distribution in the channel. They were found to be negligible.

The velocity and temperature distributions were calculated from the measured mass flow and velocity profiles for turbulent flow in a rectangular channel, and agreed well with the values measured from the $\vec{v} \times \vec{B}$ induced probe voltages recorded when no current was im-

pressed and new BN walls were used (Fig. 8). After the channel had been in operation for several hours, a conducting deposit formed on the insulating walls and lowered the measured electric field E_y. As a result of the short circuit currents I_y a Hall field E_x could then be detected.

The disturbance caused by the conducting walls could be calculated. However, even with relatively badly contaminated walls the disturbance was found to be negligible except at current densities lower than 100 mA/cm^2.

The eddy currents produced by a non-uniform $\frac{1}{n_e n} j_x B_z$ e.m.f. distribution are negligible, since the e.m.f. is nearly independent of j_x over a wide range.

As an additional check on the effects of circulating currents, we have measured σ_x and $\omega\tau$ in a current density region where no instabilities were present with the $(\vec{v} \times \vec{B})$ and $(\vec{j} \times \vec{B})$ e.m.f.'s acting in the opposite and the same direction. In this way, the e.m.f. available to drive the current in the y direction is at least doubled and errors due to circulating currents should be doubled. We have, however, found no noticeable effect.

IV. Results and discussion

The theory with simplifying assumptions predicts that the scalar electrical conductivity σ_o should be independent of a transverse magnetic field.

It was shown, however, that the momentum exchange is influenced on applying a magnetic field in cases where the cross section in collisions between electrons and heavy particles depends on the electron energy. This causes a drop in the scalar electrical conductivity $\sigma_{o \perp B \neq o}$ transverse to the magnetic field. In a fully ionized plasma it is reduced by 50 % according to R. Landshoff [12]. Corresponding calculations for a partially ionized argon-potassium mixture were made by W. Feneberg [13]. He found that the drop in conductivity, which is described by the

factor

$$\delta\,(T_e,B) = \frac{\sigma_{o\perp B\neq o}}{\sigma_{o\ B=o}}\ ,$$

was not so pronounced here as in a fully ionized gas.

This factor $\delta(T_e,B)$ decreases with increasing electron temperature and magnetic field. According to Feneberg it is between $0.89 \geq \delta(T_e,B) \geq 0.76$ for a gas temperature of $T_g = 2000\ ^oK$, a seed concentration of 0.2 % and a magnetic field $B \to \infty$ in the electron temperature range 2000 - 3400 ^oK. This smaller drop in the scalar electrical conductivity in a transverse magnetic field is due to the fact that in collisions of electrons with potassium atoms the cross section is almost independent of the electron energy, and that in collisions with argon atoms and with potassium ions the effects partially compensate one another. This is because in collisions with argon atoms the cross section increases with increasing electron energy after the Ramsauer minimum is passed, whereas in collisions with potassium ions it decreases. Besides the scalar electrical conductivity $\sigma_{o\perp B\neq o}$, Feneberg also calculated the Hall parameter $\omega\tau$ as a function of the electron temperature.

The fact that momentum exchange between electrons and heavy particles is impaired when a transverse magnetic field is applied influences the increase in the electron temperature. This influence is expressed by the factor $\delta(T_e,B)$ in the energy balance of the electrons.

Disregarding thermal conduction losses, the energy balance of the electrons is:

$$\frac{j^2}{\sigma_{o\ B=o}\ \delta(T_e,B)} = 2\, n_e \sum_j \nu_{ej}\ \frac{m_e}{m_j}\left(\frac{3}{2}\,k\,T_e - \frac{3}{2}\,k\,T_o\right) + R\,(T_e) \qquad (2)$$

ν_{ej} = mean electron collision frequency
k = Boltzmann constant
m_e = electron mass
m_j = mass of the heavy particles j
$R(T_e)$ = mean radiation loss per cm^3
n_e = electron density

$$\delta(T_e,B) = \frac{\sigma_{\perp\ B\neq o}}{\sigma_{B=o}}$$

The factor $\delta(T_e,B)$ states that with a magnetic field $B \neq 0$ the current density j would have to be reduced by a factor of $\sqrt{\delta(T_e,B)}$ in order to bring about the same electron temperature increase as with B = 0. For $B \to \infty$, $\sqrt{\delta(T_e,B)}$ is in the region $0.94 \geq \sqrt{\delta(T_e,B)} \geq 0.87$. The influence expected is therefore slight and under the given experimental conditions ($B \leq 18$ kG) it cannot be determined with certainty. This is also made difficult because the transverse magnetic field reduces the thermal conductivity of the electrons, causing a steeper electron temperature gradient near the wall with $B \neq 0$, than with B = 0. As a result, the electron temperature profile along the channel cross section changes.

Feneberg's calculations can therefore only be checked by measuring the electrical conductivity. This, however, was not possible in all ranges of current density and magnetic field, because at current densities larger than 0.1 amp/cm^2 and magnetic fields larger than 5 kG there were fluctuations in the field strengths E_x^* and E_y^*. These are caused by instabilities.

The possibility of instabilities occurring in a plasma under MHD generator conditions was first suggested by E.P. Velichov [9]. He showed that two types of instability can occur if $\omega\tau > 1$. The first is the electroacoustic instabilities or electroacoustic waves also investigated theoretically by J.E. McCune [10 et al.] and the second is the ionization instabilities or electrothermal waves. Their parameters such as growth rates and propagation velocities were calculated by J.L. Kerrebrock [11] and A.V. Nedospasov [17].

These instabilities can cause fluctuating currents $\tilde{j}$ and velocities $\tilde{v}$. When these instabilities occur the energy gain of the plasma $j \cdot E$ increases for a given current density. This additional electrical energy can lead to further ohmic heating of the plasma by the currents $\tilde{j}$ and to conversion of electrical energy into kinetic energy. In addition, the instabilities may also result in fluctuations of the scalar electrical conductivity $\tilde{\sigma}$ and the Hall coefficient $\widetilde{\omega\tau}$.

With $\sigma = \sigma_{\perp B \neq o} = \sigma_{B=o}\ \delta(T_e, B)$ the conservation of energy law is then

$$(\vec{j} + \tilde{\vec{j}})\ (\vec{E} + \tilde{\vec{E}}) = \frac{(\vec{j} + \tilde{\vec{j}})^2}{\sigma + \tilde{\sigma}} - (\vec{j} + \tilde{\vec{j}})\ \left[(\vec{v} + \tilde{\vec{v}}) \times \vec{B}\right] \qquad (3)$$

Under the given experimental conditions we have

$$j_y = j_z = E_z = v_y = v_z = B_x = B_y = 0$$

$$j_x\ ,\ E_x\ ,\ E_y\ ,\ v_x\ ,\ B_z \neq 0$$

$$\tilde{E}_x\ ,\ \tilde{E}_y\ ,\ \tilde{j}_x\ ,\ \tilde{j}_y\ ,\ \tilde{v}_x\ ,\ \tilde{v}_y \text{ may be non-zero.}$$

If there are instabilities and we get in the plasma as a result $\tilde{E}_x$, $\tilde{E}_y \neq 0$, $\tilde{v}_x$, $\tilde{v}_y \neq 0$ and $\tilde{j}_x$, $\tilde{j}_y \neq 0$, the scalar electrical conductivity and the Hall coefficient can no longer be determined with $\sigma = j_x/E_x$ and $\omega\tau = \frac{E_y - v_x B_z}{E_x}$, as described in Section III; this is because the parameters $\tilde{j}$ and $\tilde{v}$ vary with time and space and cause fluctuations of the e.m.f.'s and field strengths. These have to be allowed for in Ohm's law if the electrical conductivity σ_o and the Hall parameter $\omega\tau$ are to be measured at a given time in a given volume element. Moreover, σ and $\omega\tau$ are not constant in space and time, and so their corresponding mean values have also to be found. These measurements are not possible, however, because not even $\tilde{j}$ and $\tilde{v}$ can be determined. It is possible, however, to measure effective values of σ and $\omega\tau$ which can be defined by mean values in space and time.

$$\sigma_{eff} = \frac{\langle I \rangle / F}{\langle E_x + \tilde{E}_x \rangle} \qquad \omega\tau_{eff} = \frac{\langle E_y + \tilde{E}_y \rangle - v_x B_z}{\langle E_x + \tilde{E}_x \rangle} \qquad (4)$$

The current density is here determined from the total current I measured in the external circuit and the discharge cross section F, and the temporally constant $v_x B_z$ e.m.f. is determined from the open-circuit field. The mean values of the fields E_x, E_y are determined from the potential difference of probes 10 and 5 mm apart.

The mean values of the scalar electrical conductivity $\langle\sigma\rangle$ and of the Hall coefficient $\langle\omega\tau\rangle$ are different from their effective values, but the latter are of greater practical importance because they enable the parameters of interest in MHD generators to be given directly.

The behaviour of the electron temperature averaged in space and time is plotted in Fig. 9 as a function of the current density for magnetic fields B = 0 and B = 15 kG. The electron temperature was measured in the line wings through the middle observation window (see Fig. 3), and so it is the temperature in the centre of the channel that is given here.

From the diagram it can be seen that with the same current density the electron temperature obtained for B = 15 kG has the same value within the measuring accuracy as for B = 0. If, however, it is taken into account that the electron temperature profile with a magnetic field inside the channel is much flatter than without a magnetic field, there should with a transverse magnetic field be a slight rise compared with the values obtained without a magnetic field. The resulting differences are, however, within the limits given by Feneberg [13]. These results do not justify concluding that the fluctuating currents $\tilde{j}$ are negligible compared with the measuring current j. It is true that when fluctuating currents $\tilde{j}$ occur one would at first expect additional ohmic heating of the electrons because the component $\tilde{j}$ has also to be allowed for in the energy balance of the electrons (eq. 2). The instabilities also result, however, in fluctuations of the electron density n_e and of the electron collision frequency $\tilde{\nu}_e$ and hence of the electrical conductivity $\tilde{\sigma}$ as well. As the conductivity fluctuations $\tilde{\sigma}$ and the phase relation between $\tilde{j}$ and $\tilde{\sigma}$, $\tilde{n}_e$, $\tilde{\nu}$ are not known, however, the fact that no additional increase of the electron temperature accompanies the instabilities does not justify concluding that there are no fluctuating currents $\tilde{j}$.

Unlike the electron temperature, the effective scalar electrical conductivity σ_{eff} is strongly influenced by the magnetic field. For a given current density, σ_{eff} decreases in an argon-potassium plasma with increasing magnetic field (Fig. 10). This decrease is most pronounced between 5 and 10 kG. In this range, however, and in the ranges of current density and magnetic field in which the calculated decrease in conductivity due to the transverse magnetic field is most pronounced there are fluctuations in the field strengths E_x^* and E_y^*. Only at low current densities ($j \leq 100$ mA/cm^2), where practically no field fluctuations occur, was it possible to measure the scalar electrical

conducitvity $\sigma_{\perp B \neq 0}$. In this current density range and with increasing magnetic field a decrease in the scalar electrical conductivity was observed in agreement with the calculations.

In a helium-potassium mixture the scalar electrical conductivity was not noticeably influenced by the transverse magnetic field in the region of low current densities ($j \leq 0.4$ amp/cm^2), where no field fluctuations occur (Fig. 11). This behaviour is also in agreement with the calculations because helium does not exhibit the Ramsauer effect and the collisions between electrons and potassium ions can be ignored up to electron temperatures of 2400 ^{o}K. At current densities larger than 0.4 amp/cm^2 fluctuations in the field strengths E_x^* and E_y^* were observed. The effective scalar electrical conductivity then decreases with the magnetic field. The rise in the number of collisions between electrons and potassium ions should also become evident at this stage.

In an argon-potassium plasma the strongest deviation of the effective Hall coefficient $(\omega\tau)_{eff}$ from the theoretically expected behaviour also occurs at the same magnetic field strengths (5 - 10 kG), where the decrease in the effective scalar electrical conductivity is most pronounced (Fig. 12). If $(\omega\tau)_{eff}$ is plotted as a function of the magnetic field, the expected linear dependence of the magnetic field occurs only at low current densities and low magnetic fields. In agreement with the behaviour of the effective scalar conductivity values, the effective values of the Hall coefficients measured for high magnetic fields and current densities are much lower than those calculated by Feneberg. In the range investigated they are practically constant for high magnetic fields. These results agree with the measurements of R. Dethlefsen and J.L. Kerrebrock [18] and V.N. Belonsov, V.V. Eliseev and I.Ya. Shipuk [19], who under similar conditions also observed field fluctuations, which they ascribed to ionization instabilities. In the region in which $\omega\tau$ is a linear function of the magnetic field the deviations from the values calculated by Feneberg do not exceed 10 %. The expected decrease of the Hall coefficient with increasing electron temperature was confirmed.

The marked decrease of the effective conductivity values and the effective Hall coefficients only occurs when field fluctuations can be observed. This means that the instabilities lead to increased input

of electrical energy, which is dissipated in the plasma. As the electron temperature measurements showed, however, these instabilities do not cause any appreciable increase in ohmic heating of the electrons. It can therefore be assumed that electrical energy is essentially converted into kinetic energy as a result of the instabilities. In evaluating this statement, however, allowance should be made for the fact that all measuring results are values averaged in time and space.

V. Fluctuation measurements

At low current densities ($j \sim 100$ mA/cm^2) the field fluctuations were mainly in the direction of the current flow. It was not possible in this region to observe defined frequencies. When the current density was increased and the ratio of electron temperature T_e to gas temperature T_o, T_e/T_o, exceeded the value 1.2, the amplitude of the Hall field fluctuations E_y^* increased in proportion to that of E_x^*. Furthermore, there was a well-defined frequency which in the range of current density and magnetic field investigated was between 7 and 10 kHz.

In Fig. 13 E_x^* and E_y^* are plotted as a function of time for a current density of $j = 1$ amp/cm^2 and a magnetic field of 5 kG. In the oscillograms well-correlated fluctuations with a frequency of $\nu = 7 \pm 1$ kHz can be observed. Correlated field fluctuations occurred only in a $\omega\tau$-range $2 \leq \omega\tau \leq 3.5$. With rising $\omega\tau$-values and electron temperature there was an increase in the frequency of the potential fluctuations. The frequency spectrum contained in the oscillations also spread, and relationships between the individual probe signals could no longer be ascertained. With increasing T_e/T_o the amplitude of the fluctuations also increases. In the region of correlated fluctuations there may be macroinhomogeneities as found by V.V. Belonsov et al. [19], who observed regular striations in the discharge in the corresponding $\omega\tau$-region. If the $\omega\tau$-values are increased, those macroinhomogeneities become microinhomogeneities. With the set-up used here, however, it was not possible to make the measurements necessary for investigating the striation structure. The oscillograms (Fig. 13) allow the propagation velocities V_x' and V_y' of the waves in the x and y-direction respectively to be measured. Since the flow velocity of the plasma v_x

is known, the following relations

$$V'_x = v_x + u \sin \alpha \tag{4}$$

$$V'_y = v_x \operatorname{tg} \alpha + u \cos \alpha \tag{5}$$

can be used to determine the phase velocity u relative to the plasma and the direction of the wave vector $\vec{K}$. The values obtained from the oscillograms are shown in Table 1. The $\omega\tau$-values were determined here by extrapolating the values obtained in the lower magnetic field region, where the $\omega\tau$-values are still a linear function of the magnetic field (Fig. 12).

$\omega\tau$	T_e °[K]	u [m/sec] measured	u [m/sec] calculated	α measured	α' calculated
2.2	2750	-30 ±12	19	35 ± 3°	33°
3.3	2750	-33 ±10	19	36 ± 4°	37°

Table 1

The phase velocity of an electrothermal wave was given by J.L. Kerrebrock [11] and A.V. Nedospasov [17], and is

$$U = \frac{\omega}{K} = \frac{kT_e \, j_o \cos \alpha'}{U_i \, e \, n_{eo}} \tag{6}$$

Here α' gives the angle between the direction of the current j_{ox} and the wave front. kT_e and U_i are the electron temperature and the ionization energy respectively, expressed in eV. The subscript o denotes the unperturbed parameters. The angle α' introduced is identical with the measured angle α; this is because it was assumed in the calculations that rot E = 0 and div j = 0. It follows from this that $\vec{E} \times \vec{K} = 0$ and $\vec{j} \times \vec{K} = 0$.

A.M. Dykhne determined for electrothermal waves a relation between the angle α' and the Hall coefficient $\omega\tau$. This relation is given in [19]:

$$\operatorname{tg} \alpha' = \frac{\sqrt{1 + (\omega\tau)^2} - 1}{\omega\tau} \tag{7}$$

To calculate the angle α' the extrapolated $\omega\tau$-values were used in eq.(7).

Comparison of the measured values with the values calculated for electrothermal waves shows good agreement. As postulated, it held in all cases that $K_y/K_x < 0$, where K_x and K_y are the components of the wave vector $\vec{K}$ along the current j_{ox} and along the Hall field strength E_y determined by $-\frac{1}{n_e e}(j_{ox} B_z)$.

From these results and the fact that the amplitude of the field fluctuations increases with increasing T_e/T_o, it may be concluded, in agreement with the authors already quoted [18, 19], that the fluctuations are due to electrothermal waves.

For low current densities ($j < 100$ mA/cm^2), $n_e < 10^{13}$/cm^3 and $\omega\tau \leq 2$ field fluctuations were only found in the x-direction. The amplitude fluctuations were less than 50 % of the mean value of E_x. The probe signals showed a correlation (Fig. 14). It was concluded from the signals that these waves propagate in the plasma antiparallel to the direction of the current with a phase velocity of $u = 50$ m/sec. The direction of propagation of these waves corresponds to that of magnetoacoustic waves. The propagation velocity measured here, however, is an order of magnitude lower than that calculated. Superposing magnetoacoustic waves propagating in opposite directions may result, however, in a propagation velocity such as was measured here. It may therefore be assumed that the waves occurring at $T_e/T_o < 1.2$ are magnetoacoustc waves.

The conductivity and Hall coefficient were also measured for a channel cross section of 1.3 cm^2. With this cross section there was, however, no possibility of checking the isotropy of the current density distribution and correcting it, if necessary. The results obtained for this geometry are therefore only to be regarded as a rough limit below which the actual conductivity values do not drop.

The Hall coefficients determined for this channel cross section also have a saturation value, but it is about a factor of 2 above the value found for a cross section of 3 cm^2. There were no appreciable differences in the conductivity values. The field fluctuations were much less pronounced, however, than in the case of the larger channel cross section.

But these results can only show the general trend. To obtain more exact information on the influence of the geometry on the development of the instabilities, measurements have to be made with a larger number of channel cross sections. Such measurements are planned.

VI. Conclusions

The electrical conductivity and the Hall coefficient were measured in rare gas alkali plasmas with crossed electric and magnetic fields and macroscopically isotropic current density distribution. The results show that in an argon-potassium mixture with current densities and magnetic fields in which $T_e/T_g < 1.2$ ($T_o = 2000\ ^oK$) and $\omega\tau < 2$ the values of the scalar electrical conductivity and the Hall coefficient confirmed those calculated by W. Feneberg. As expected, the scalar electrical conducitvity in the argon-potassium mixture decreased with increasing magnetic field. But in a helium-potassium mixture it was constant, which was also to be expected from the theory.

If $T_e/T_g > 1.2$ and the Hall coefficient is $\omega\tau > 2$, there occur electrothermal waves, which allow only effective conductivity values and Hall coefficients to be measured. The effective scalar electrical conductivity then decreases strongly with increasing magnetic field, particularly in the region of 5 to 10 kG, whereas the effective Hall coefficient has a constant value between 2 and 3. In the region $2 \leq \omega\tau \leq 3.5$ there were well-correlated field fluctuations which enabled the phase velocity and the direction of propagation of the waves to be measured. The reduction of the scalar electrical conductivity and Hall coefficient and the amplitude of the field fluctuations depend on the geometry of the measuring channel, as was shown by measurements using various channel cross sections.

Acknowledgments

We should like to thank Prof. Dr. Wienecke for his interest and support. Appreciation is also due to several colleagues, particularly Dr. Salvat, for valuable discussions. We also wish to thank R. Borde, W. Breitfeld and P. Reinhold, who set up and supervised the measuring apparatus.

References

1 KERREBROCK, J.L., "Conduction in Gases with Elevated Electron Temperature", Engineering Aspects of Magnetohydrodynamics (Columbia Univ. Press, New York, 1962, pp. 327-346)

2 ZUKOSKI, E.E., COOL, T.A., GIBSON, E.G., "Experiments Concerning Nonequilibrium Conductivity in a Seeded Plasma", AIAA J., Vol. 2, 1410-1417 (1964)

3 KERREBROCK, J.L., HOFFMANN, M.A., "Nonequilibrium Ionization Due to Electron Heating: II. Experiments", AIAA J., Vol. 2, 1080-1087 (1964)

4 COOL, T.A., ZUKOSKI, E.E., "Recombination, Ionization and Nonequilibrium Electrical Conductivity in a Seeded Plasma", Phys. Fluids, Vol. 9, 780-796 (1966)

5 RIEDMULLER, W., "Measurements of Electron Temperature in an Argon-Potassium-Plasma", Inst. f. Plasmaphysik, Garching, Rep. IPP 3/31 (1965)

6 GOLUBEV, V.S., KASABOV, G.A., KONAKH, V.F., "Study of a Steady-State Ar-Cs-Plasma with Nonequilibrium Conductivity", High Temp. Vol. 2, 445-459 (1964) transl. from Teplofizika Vysokikh Temperatur, Vol. 2, 493-509 (1964)

7 HURWITZ, H., KILB, R.W., SUTTON, G.W., "Influence of Tensor Conductivity on Current Distribution in a MHD Generator", J. Appl. Phys., Vol. 32, 205-216 (1961)

8 KERREBROCK, J.L., "Segmented Electrode Losses in MHD Generators with Nonequilibrium Ionization", AIAA J., Vol. 4, 1938-1947 (1966)

9 VELICHOV, E.P., "Hall Instability of Current Carrying Slightly Ionized Plasma", Symp. on MHD Electr. Power Gen., Newcastle upon Tyne, Paper 47 (1962)

10 McCUNE, J.E., "Wave Growth and Instability in Partially Ionized Gases", Symp. on MHD Electr. Power Gen., Paris, Paper No. 33 (1964)

11 KERREBROCK, J.L., "Nonequilibrium Ionization Due to Electron Heating, I. Theory", AIAA J., Vol. 2, 1072-1080 (1964)

12 LANDSHOFF, R., "Transport Phenomena in a Completely Ionized Gas in Presence of a Magnetic Field", Phys. Rev., Vol. 76, 904 (1949)

13 FENEBERG, W., "The Electrical Conductivity of a Partially Ionized Argon Potassium Plasma in a Magnetic Field", Z. f. Naturf., Vol. 21a, 1468 (1966)

14 STRONG, H.M., BOUNDY, F.P., "Measurement of Temperatures in Flames of Complex Structure by Resonance Line Radiation", J. Appl. Phys., Vol. 25 Nr. 12, 1520-1537 (1954)

15 RIEDMULLER, W., SALVAT, M., "Determination of Electron Temperature by Means of the Line Reversal Method", 7th Int. Conf. on Phen. in Ionized Gases, Belgrade (1965)

16 GORENFLO, R., HERTWECK, F., PACCO, M.G., "Calculation of the Current Flow Directions in a Channel with Staggered Electrodes under MHD Generator Conditions", Inst. f. Plasmaphysik, Garching, Rep. in preparation

17 NEDOSPASOV, A.V., "Speed of Ionization Waves in Low Temperature Plasma", Int. Symp. on MHD Elec. Power Generation, Salzburg (1966) paper SM-74/97

18 DETHLEFSEN, R., KERREBROCK, J.L., "Experimental Investigation of Fluctuations in a Nonequilibrium MHD Plasma", Seventh Symp. on Engin. Aspects of Magnetohydrodynamics, p. 117 (1966)

19 BELOUSOV, V.V., ELISEEV, V.V., SHIPUK, K.Ya., "Ionisation Instability and Turbulent Conductivity of Nonequilibrium Plasma", Int. Symp. on MHD Elec. Power Generation, Salzburg (1966) paper SM-74/88

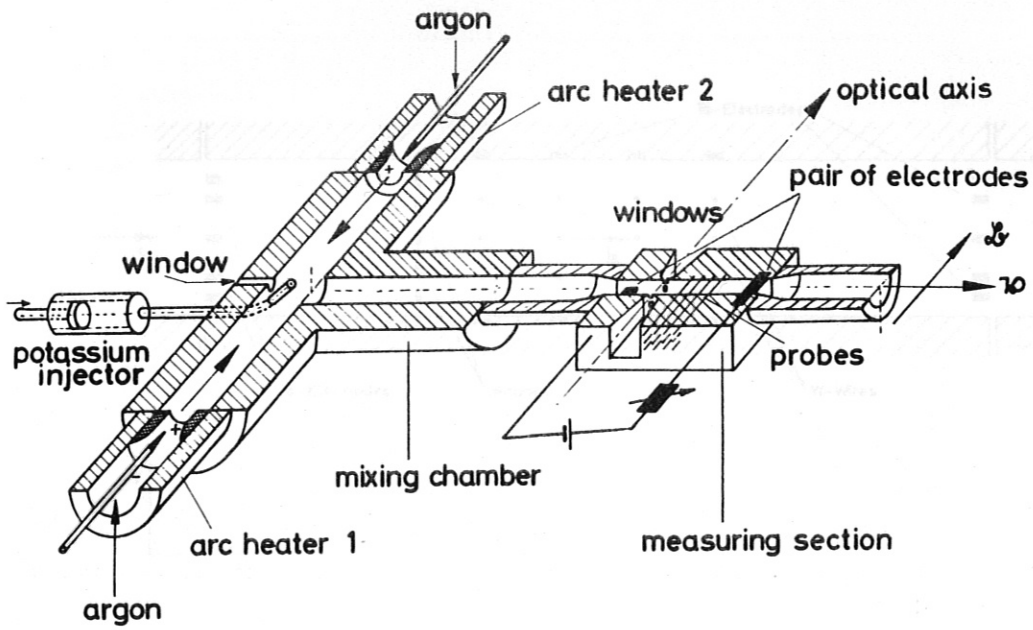

Fig. 1 Diagram of the equipment.

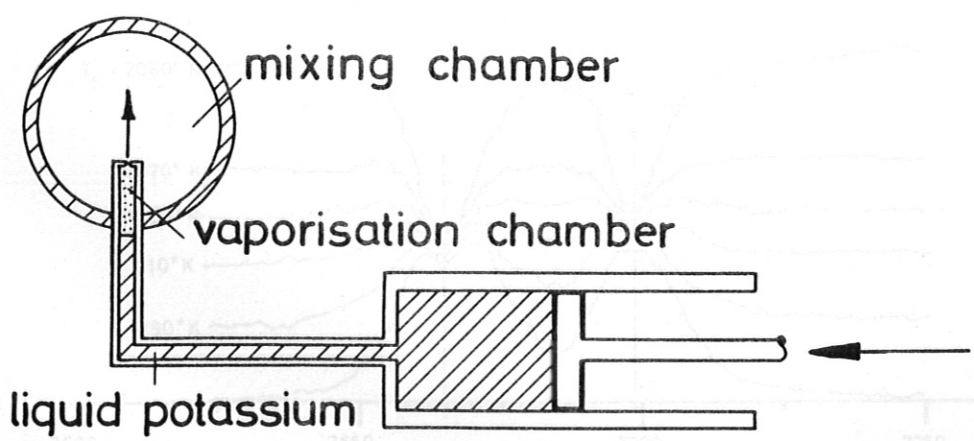

Fig. 2 Potassium injection system.

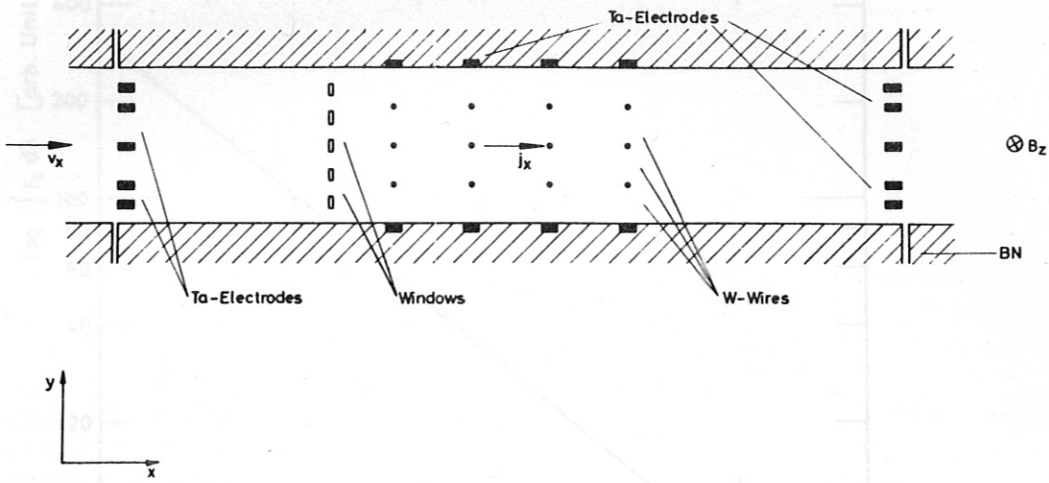

Fig. 3 Measuring channel diagram .
The channel is 100 mm long, 20 mm high and 15 mm wide. The windows are 1.6 mm long and 0.6 mm wide. The tungsten wires are 0.5 mm in diameter.

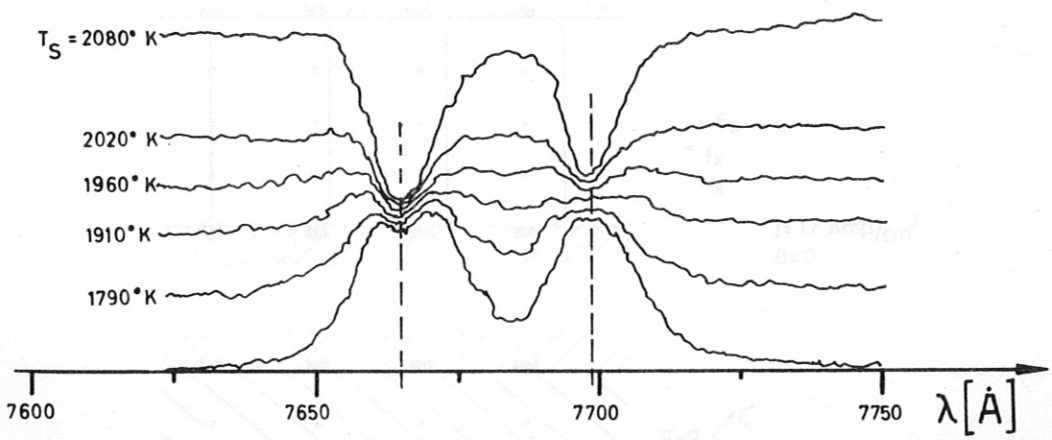

Fig. 4 The potassium resonance doublet for different radiation intensities of strip lamp $B_\lambda(T_B)$.

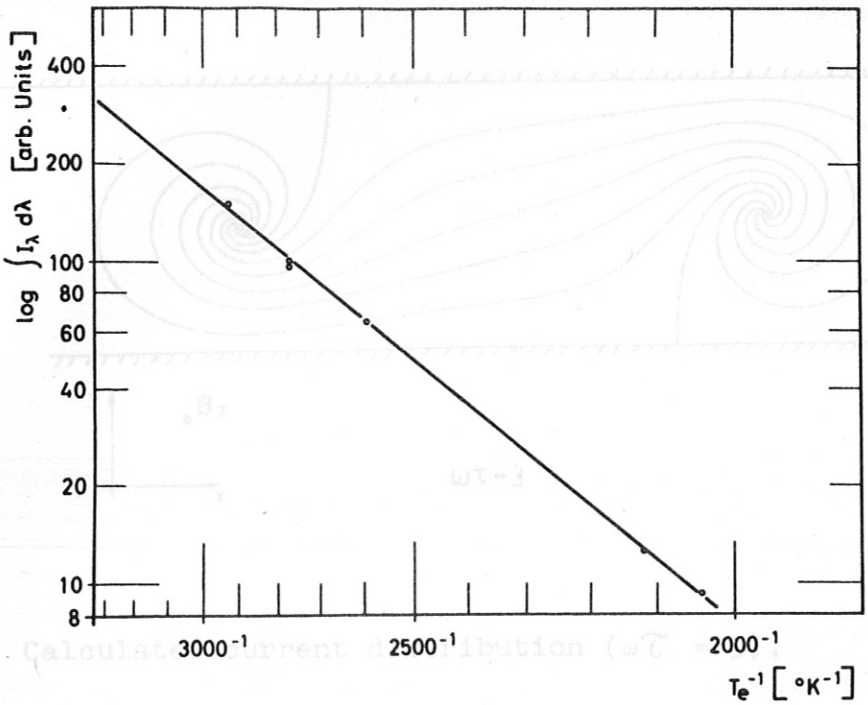

Fig. 5 log $\int I_\lambda d\lambda$ integrated over both potassium resonance lines plotted as a function of the measured $^1/T_e$.

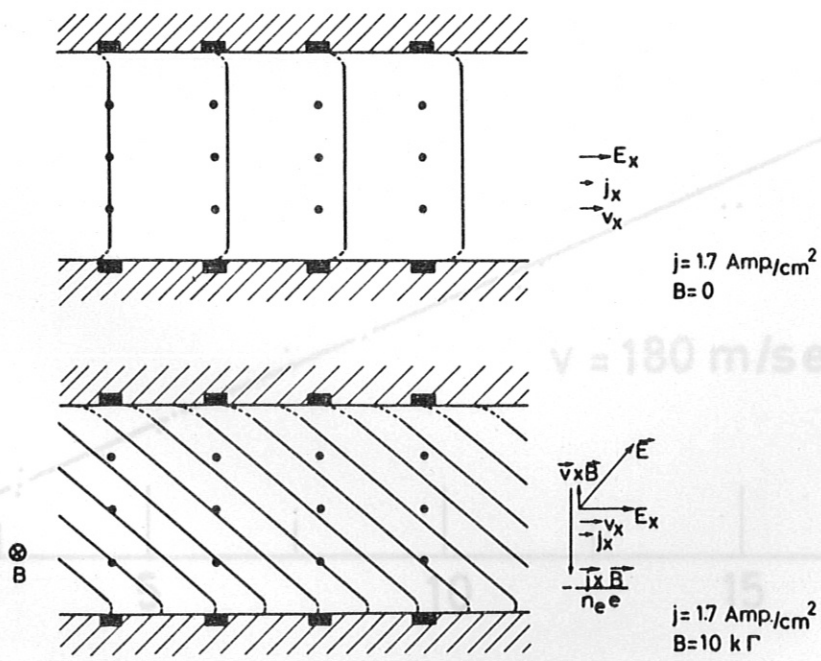

Fig. 6 Measured potential distributions with and without magnetic field.

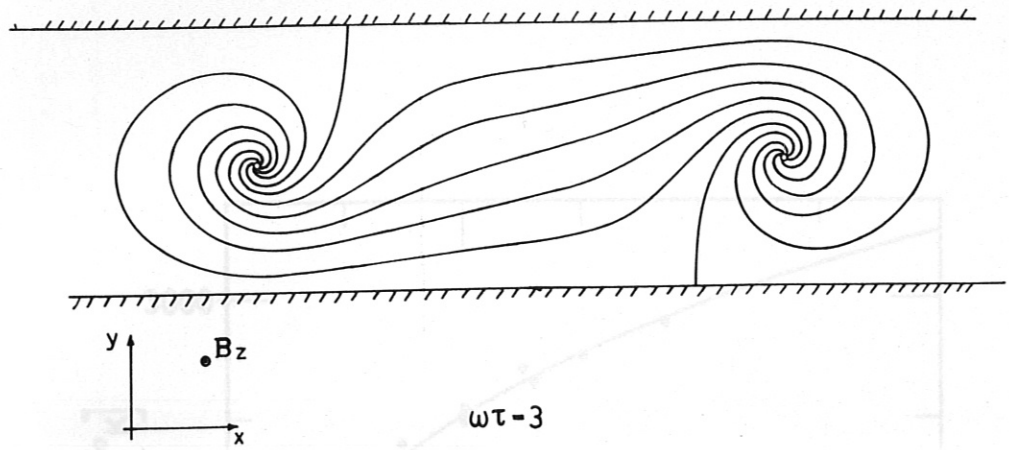

Fig. 7 Calculated current distribution ($\omega\tau = 3$).

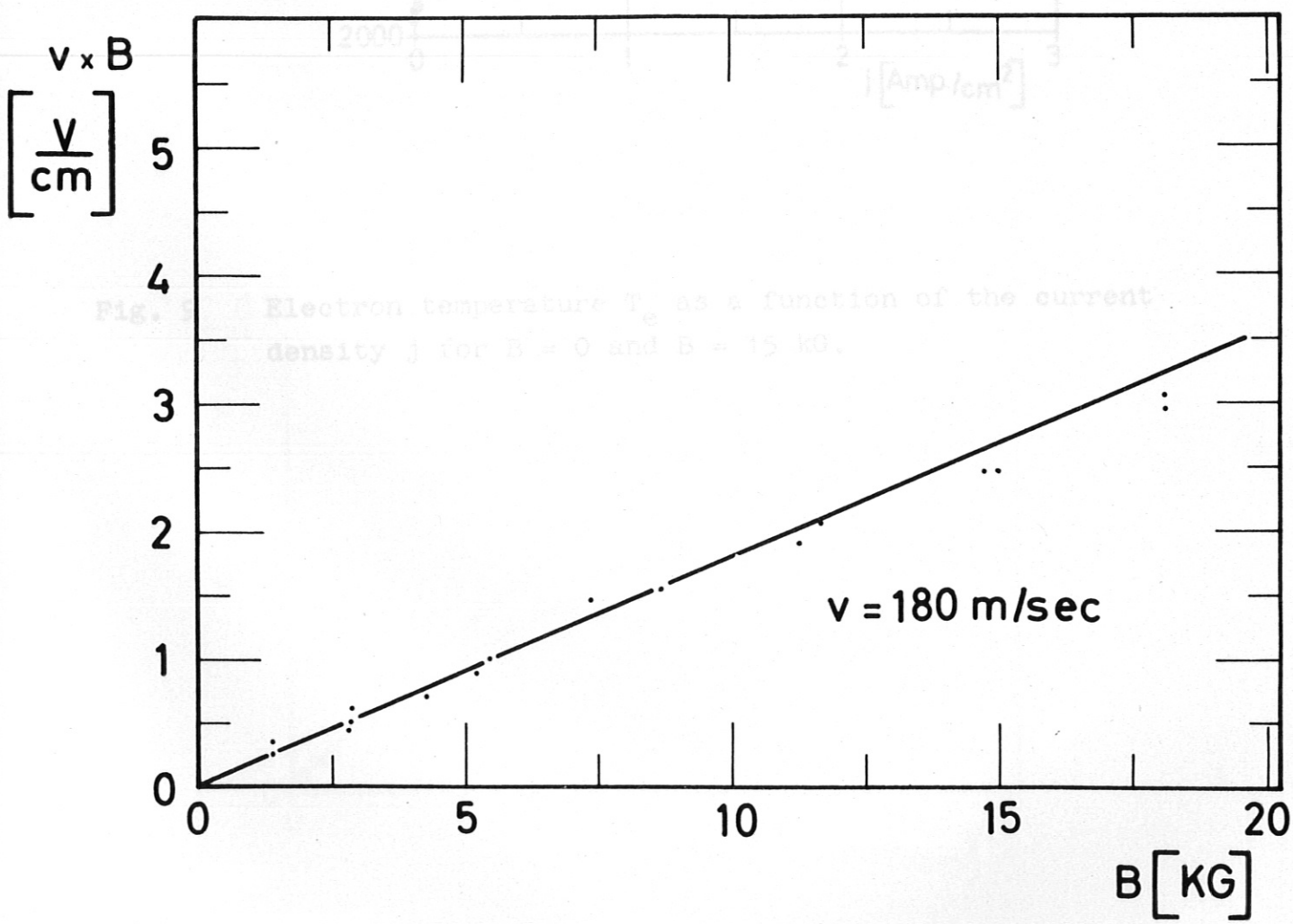

Fig. 8 Open circuit field strength as a function of the magnetic field B.

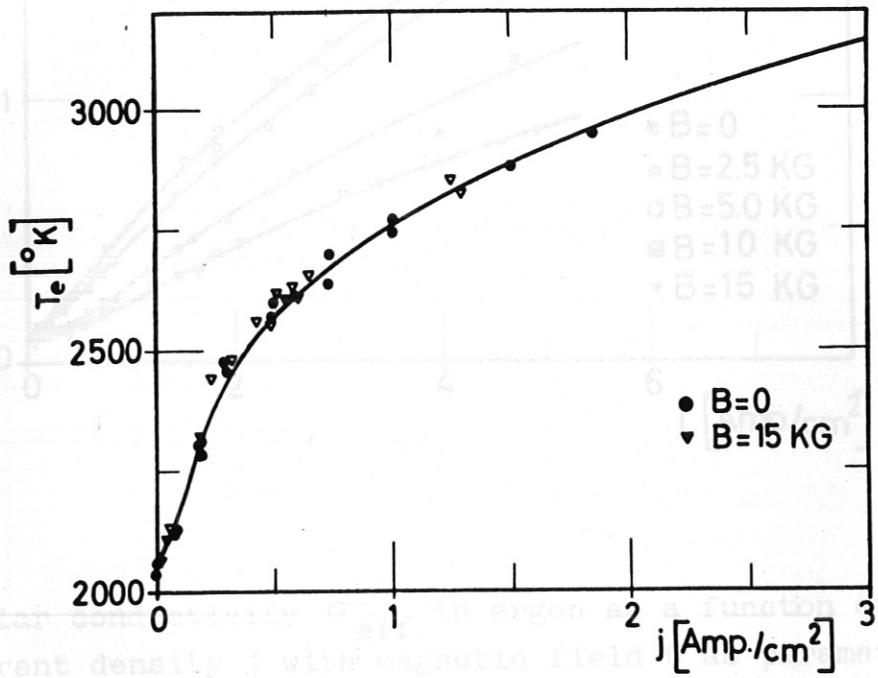

Fig. 9 Electron temperature T_e as a function of the current density j for B = 0 and B = 15 kG.

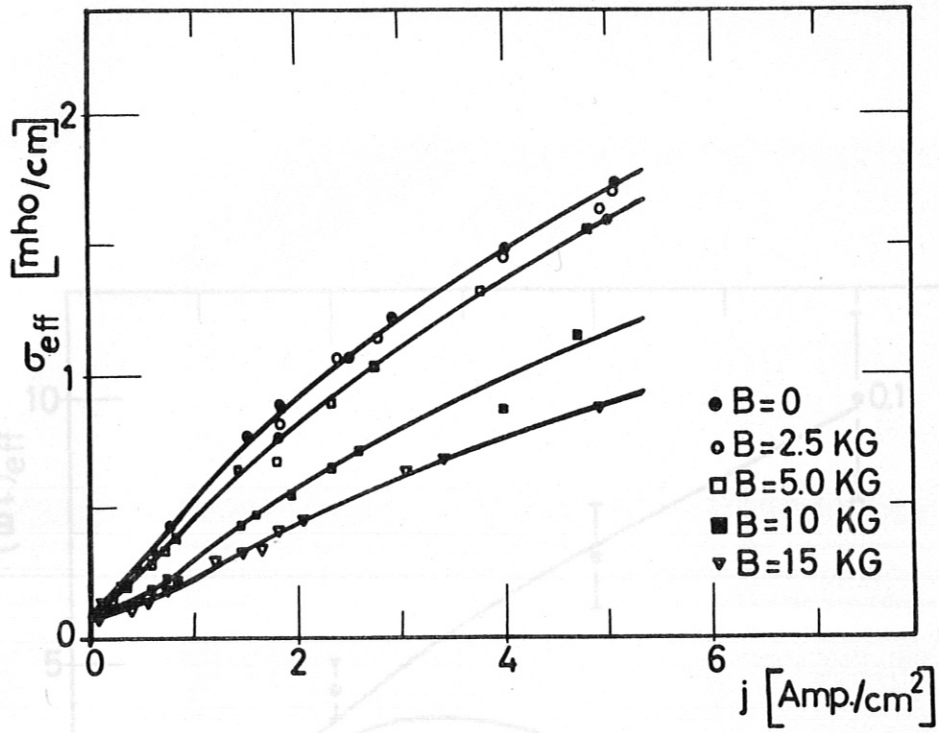

Fig. 10 Scalar conductivity σ_{eff} in argon as a function of the current density j with magnetic field B as parameter.

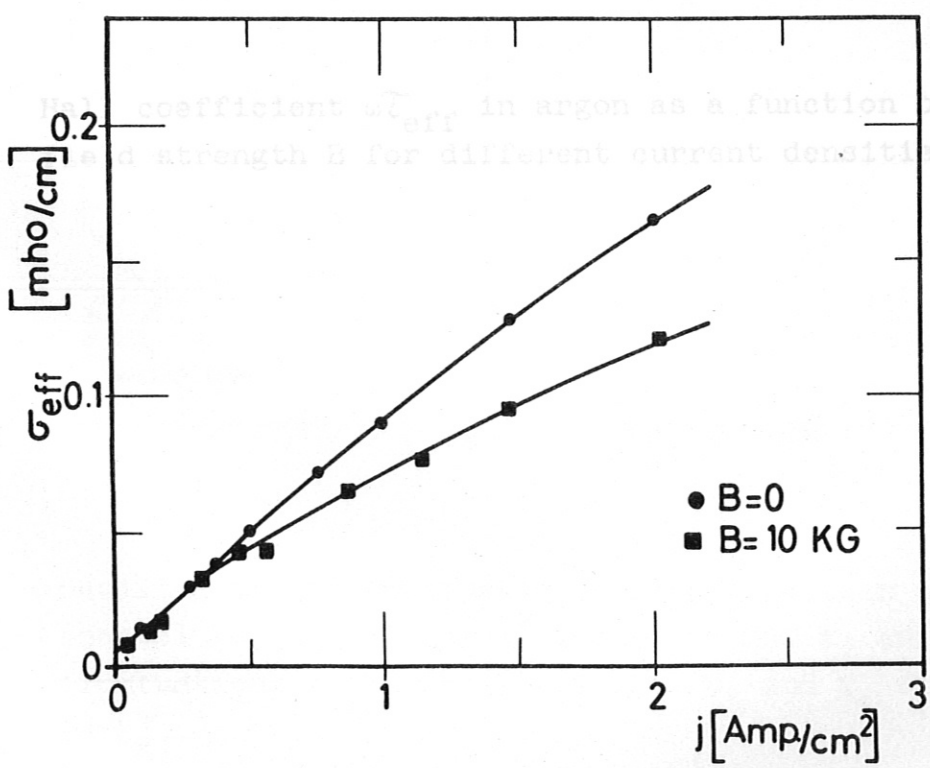

Fig. 11 Scalar conductivity σ_{eff} in helium as a function of the current density j for B = 0 and B = 10 kG.

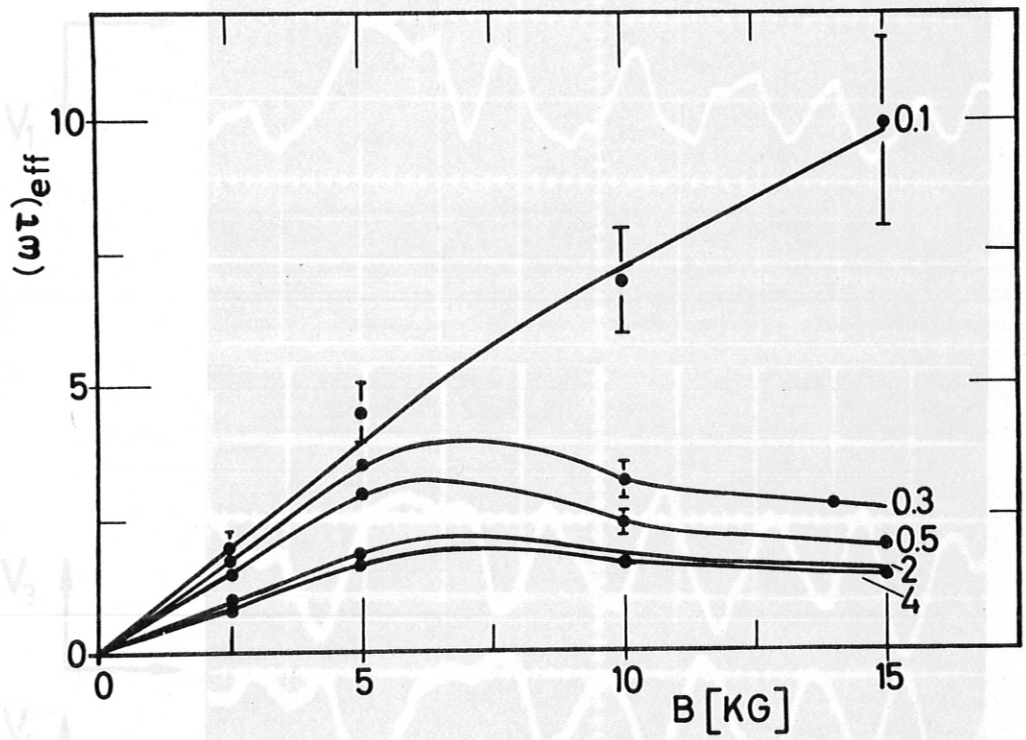

Fig. 12 Hall coefficient $\omega\tau_{eff}$ in argon as a function of magnetic field strength B for different current densities j [amp/cm^2]

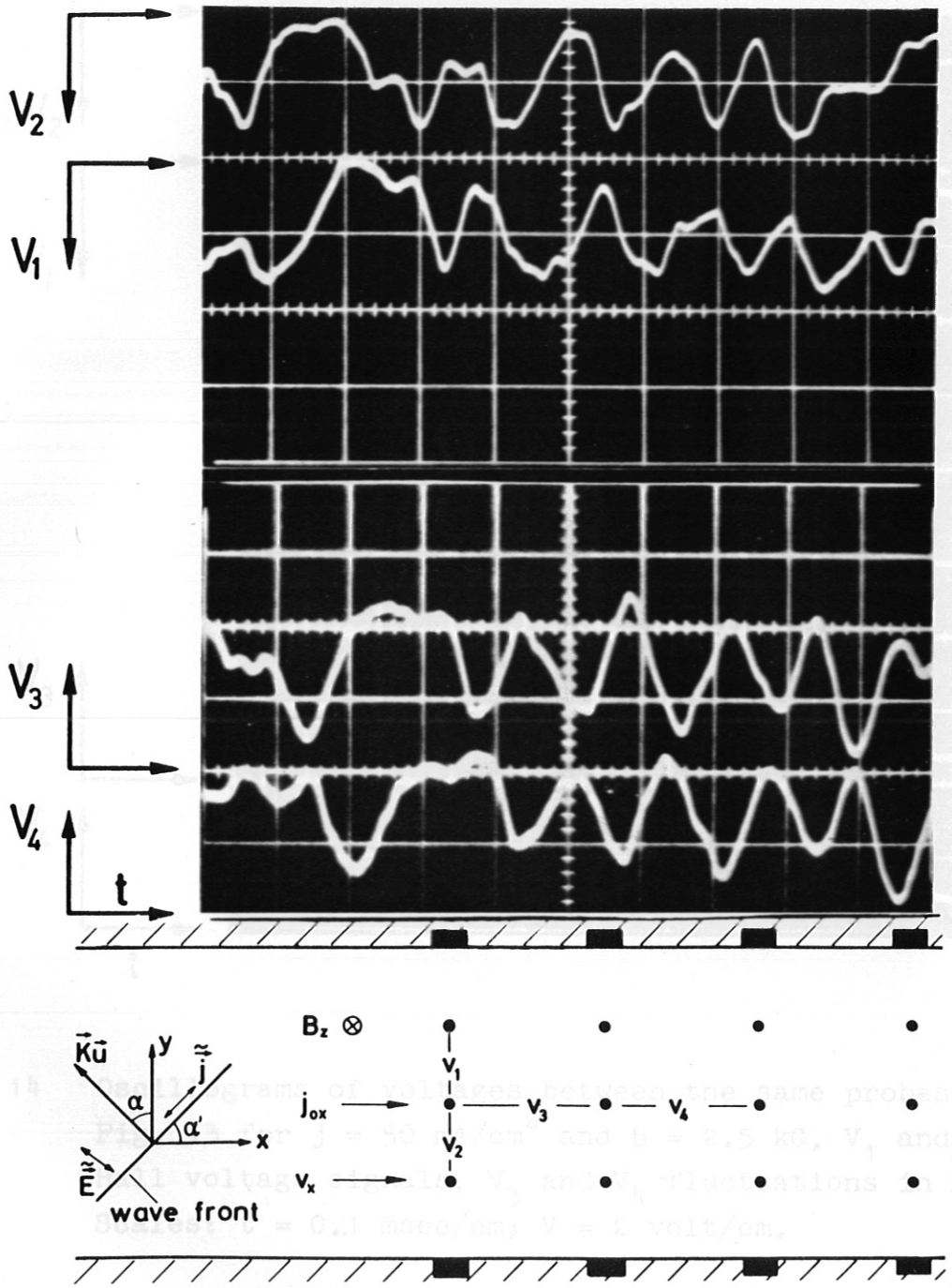

Fig. 13 Oscillograms of fluctuating voltages between probes in the channel for j = 1 amp/cm^2 and B = 5 kG, V_1 and V_2 fluctuations in E_y^* (Hall voltage) V_3 and V_4 fluctuations in E_x^*.
Scales: t = 0.1 msec/cm; V = 2 volt/cm.

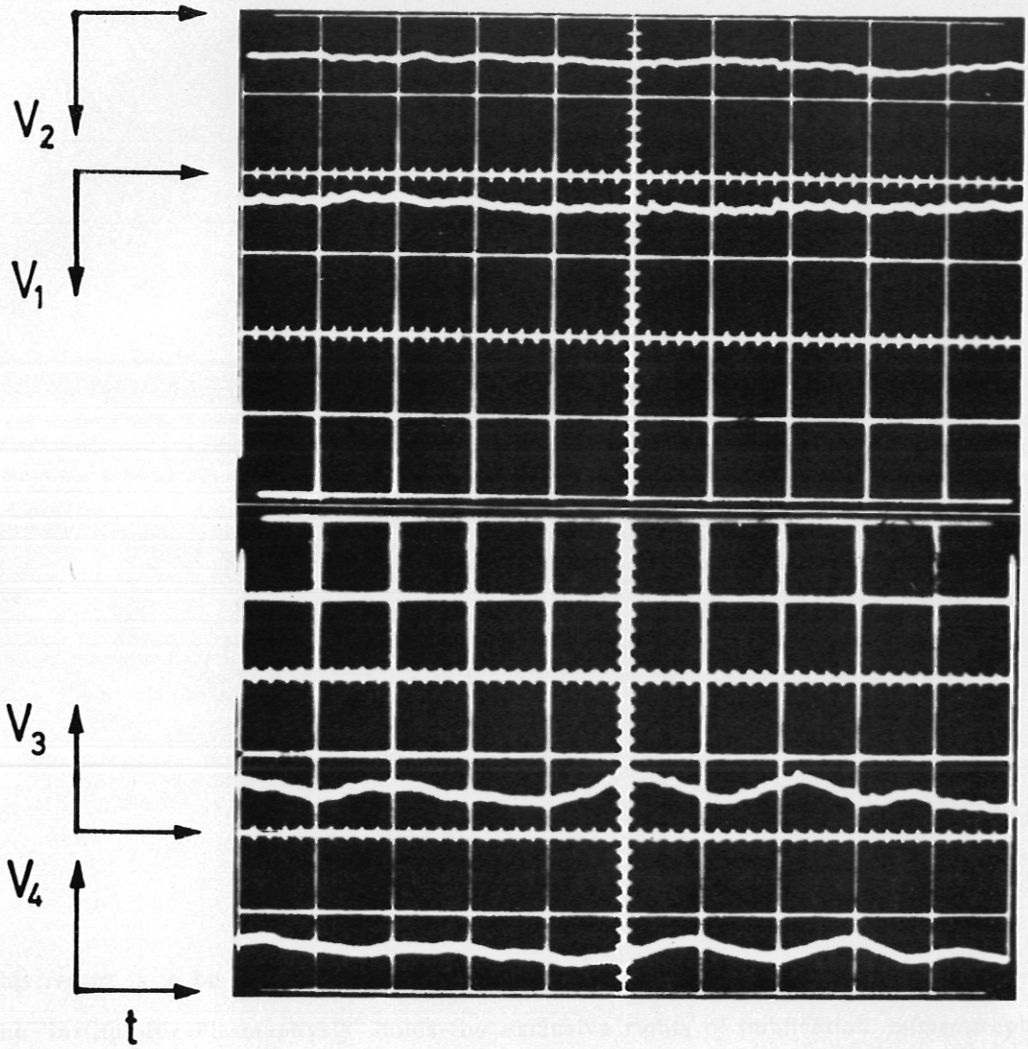

Fig. 14 Oscillograms of voltages between the same probes as in Fig. 13 for $j = 50$ mA/cm^2 and $B = 2.5$ kG, V_1 and V_2 Hall voltage signals, V_3 and V_4 fluctuations in E_x^*. Scales: $t = 0.1$ msec/cm; $V = 2$ volt/cm.